



Dynamic behavior of laterally loaded caisson foundations based on different cushion types: an experimental and theoretical study*

Wen-bo TU^{†1}, Mao-song HUANG^{2,3}, Xiao-qiang GU^{2,3}

¹School of Civil Engineering and Architecture, East China Jiaotong University, Nanchang 330013, China

²Department of Geotechnical Engineering, Tongji University, Shanghai 200092, China

³Key Laboratory of Geotechnical and Underground Engineering of Ministry of Education, Tongji University, Shanghai 200092, China

[†]E-mail: wenbotu@126.com

Received Aug. 14, 2019; Revision accepted Jan. 14, 2020; Crosschecked June 15, 2020

Abstract: Bridge foundations located in deep water are usually subjected to horizontal dynamic loads and moments which may be caused by the wind, waves, earthquake, and the possibility of boat crashing or vehicle braking. Caisson foundations based on gravel or sand cushions are a new type of deep-water foundation for bridges, suitable for meizoseismal areas. In this paper, harmonic horizontal excitation tests for the study of the lateral dynamic response of caisson foundations based on cushion layers are described. Different lateral loads and two different cushion types are considered. The results show that the lateral dynamic responses of caisson foundations based on sand and gravel cushions both show strong nonlinear characteristics, and the resonant frequency of the foundation decreases with the increase of the excitation force. The dynamic displacement of a foundation based on a sand cushion is far less than that based on a gravel cushion, and the rate of decrease of the resonant frequency of a foundation based on a gravel cushion is faster than that of a foundation based on a sand cushion under the same conditions. Under dynamic loading the gravel cushion can more effectively dissipate vibration energy and isolate the vibration, than the sand cushion can. A simplified nonlinear analysis method is proposed to simulate the lateral dynamic response of caisson foundations, and the predicted response shows a reasonable match with the results observed in laboratory tests. Scaling laws have also been applied in this small-scale vibration model test to predict the dynamic behavior of the prototype foundation.

Key words: Nonlinear dynamic response; Caisson foundation; Harmonic vibration test; Gravel cushion; Sand cushion
<https://doi.org/10.1631/jzus.A1900381>

CLC number: TU435

1 Introduction

Cross sea or river bridge foundations located in deep-water are usually subjected to the horizontal dynamic loads and moments. The horizontal dynamic loads and moments may be caused by long-term cyclic load and transient load, such as the wind, waves,

earthquake, and the possibility of boat crashing or vehicle braking. Choosing the proper type of bridge foundation to bearing the vertical forces and ensuring the performance subjected to lateral loads is critical for the bridge safety. The caisson is a deep-water bridge foundation type which is suitable for offshore engineering, and a damping material is usually laid on its foundation base to improve its seismic performance (Combault, 2011). When lateral vibration occurs, the cushion layer will gradually change from the elastic stage to the plastic stage with a plastic deformation concentrated on the foundation base. Two cushion materials are typically used in engineering practice: sand and gravel. A sand cushion has the advantages of low cost, long durability, and easy

* Project supported by the National Natural Science Foundation of China (Nos. 51808220 and 51822809), the Natural Science Foundation of Jiangxi Province (Nos. 20192BAB216036 and 20181BCB24011), and the Science and Technology Research Project of the Education Department of Jiangxi Province (No. GJJ180340), China

 ORCID: Wen-bo TU, <https://orcid.org/0000-0003-2879-6584>

© Zhejiang University and Springer-Verlag GmbH Germany, part of Springer Nature 2020

availability. Li (1989) first proposed the isolation and energy dissipation technology with a sand cushion as the isolation layer, and successfully applied it to a four-story isolation house in Beijing, China. Then, other researchers suggested that adding rubber and asphalt would improve the sand cushion (Shang et al., 2009; Liu et al., 2017). However, this research was mainly focused on the reduction of response in the building. There is also extensive research on the characteristics of a gravel cushion, but it is focused on its vertical performance as a treatment method for composite foundations (Liang et al., 2003; Ghalesari and Rasouli, 2014; Han et al., 2016).

A gravel cushion under a caisson foundation for vibration isolation was first used in the Rion-Antirion bridge in 2004 (Qian, 2004). The four pylons of the main bridge simply rest on gravel cushion layers through concrete caisson foundations with a diameter of 90 m (Combault, 2011; Zhu et al., 2014). Infanti et al. (2004) carried out a full-scale testing to study the characteristics of the seismic dissipation system used for the bridge. Combault et al. (2000) and Pecker and his co-authors (Pecker and Teyssandier, 1998; Pecker, 2004) discussed the seismic response of its superstructure. Chen et al. (2018) conducted a series of $1g$ model tests (where g is the acceleration of gravity) to study the characteristics of bearing capacity and displacement of the caisson foundation on a gravel cushion subjected to lateral static load, cyclic load, and static loads after cyclic loading. However, few studies have investigated the cushion layer effect on the response of the foundation, especially the lateral dynamic response. Moreover, the selection of the cushion type under the caisson base is one of the important issues of engineering design, and in addition to vertical loads, the cushion layer is usually exposed to waves and strong wind more than to seismic loads and it is, therefore, necessary to pay more attention to its performance under lateral dynamic loads and to analyze the effect on the dynamic response of the upper foundation or superstructure.

Due to the lack of experimental data for the design and lateral dynamic performance of this type of foundation, horizontal harmonic excitation laboratory tests were conducted to investigate the effect of different cushion types on the horizontal vibration characteristics of the caisson foundations and to assess the influence of various load amplitudes on their lateral

dynamic response. According to the experimental results, a simplified method for calculating the lateral dynamic response of caisson foundations based on the gravel cushion or the sand cushion is proposed using the nonlinear dynamic Winkler model. Comparison of the experimental results with the theoretical results is reported and discussed to reveal the isolation and energy dissipation mechanism of the foundation and to provide a reference for its engineering application. Moreover, the mechanical properties between the prototype and model foundation are established by a scaling law for $1g$ model test, which can provide a reference for engineering application.

2 Experimental set-up

In order to obtain the lateral dynamic characteristics of a foundation based on different cushion types, this study takes the foundations of the Greek Rion-Antirion bridge as the prototype (Qian, 2004; Combault, 2011), and two series of $1g$ horizontal harmonic excitation laboratory tests were conducted on them.

2.1 Model description

The caisson foundation of the Rion-Antirion bridge is simply placed on a gravel cushion layer without any connections, as shown in Fig. 1.

The gravel cushion layer consists of a 50-cm thick soil filter layer, a 200-cm thick cobble layer with particle size of 10–80 cm, and a 50-cm thick gravel layer (Dong and Zhou, 2004; Wang et al., 2017). The foundation diameter of the bridge is 90 m, which is significantly larger than the thickness of the layers and the particle size. Therefore, a uniform scale is not proper for the dynamic test and different model scales between horizontal and vertical directions are designed under the criteria provided by Dou (2001). The horizontal scale, λ_L , and vertical scale, λ_H , were determined as 375 and 300, respectively. In fact, the cushion layer beneath the caisson foundation is always below the water surface. However, it is not possible to perform the vibration test in water due to that the test equipment is not waterproof. Based on the similarity theory, the particle scale is used to consider the characteristics of soil in water, such as the kinematic characteristic of soil under the wave or

earthquake loading. The particle scale, λ_d , can be calculated by (Dou, 2001; Wang et al., 2017)

$$\lambda_d = \frac{\lambda_v^2}{\lambda_c^2 \times \lambda_m}, \quad (1)$$

where λ_v is the velocity scale, which is equal to 17.32; λ_m is the material scale, which is equal to 1.65; λ_c is the relative scale, which is equal to 1.118.

A geometrical scaling factor λ_N was determined as 375, which is equal to λ_L , for the caisson model foundation. The dimensions of the caisson model are shown in Fig. 2. The caisson model is composed of two hollow aluminum cylinders, and the hollow part is filled with concrete. The total mass of the model foundation is 3.34 kg, which corresponds to the average vertical stress of 0.74 kPa at the caisson base. The material scale is also a main factor in a small-scale model. The density scaling factor used for the 1g model test λ_p was determined as 1.0. The strain scaling factor used for the 1g model test λ_e was determined as $\lambda_N[(V_s)_m/(V_s)_p]^2$, where $(V_s)_m$ and $(V_s)_p$ are the shear velocities of soil deposits in the model container and the prototype, respectively (Iai and Sugano, 1999). The shear wave velocities can be measured by the in-situ test (Hall and Bodare, 2000) or laboratory test (Gu et al., 2015). Silty sand was used in the laboratory test. The mean particle diameter of the silty sand d_{50} is 0.15 mm. The maximum and minimum void ratios of the soil are 1.004 and 0.685, respectively. The minimum and maximum dry densities of the soil are 1322 kg/m³ and 1573 kg/m³, respectively. Before the tests, the sand was placed and hand-packed in the container in several 10-cm thick layers. The density of each soil layer is 1500 kg/m³. During the tests, the model foundation is placed directly on the sand cushion or the gravel cushion. It can be assumed that the bottom of the foundation is not connected to the soil and relies only on friction to provide lateral resistance. The thickness of each soil layer is shown in Table 1, and the diameter of the cushion gradually increases from top to bottom in a truncated cone shape. The thickness of the gravel layer, cobble layer, and filter layer are 1.7 mm, 6.7 mm, and 1.7 mm, respectively. The relative position of each layer at the bottom of the caisson can refer to Fig. 1. The particle diameters of the gravel layer and cobble layer are calculated to be 2.1 mm and

5.5 mm, respectively. Since the filter layer in prototype is composed of sand with small particle size (Dong and Zhou, 2004), the filter layer in model test is replaced with the silty fine sand, which is the same as the sand used in the vibration test in the container. The diagrams of model foundation and gravel cushion are shown in Figs. 3 and 4.

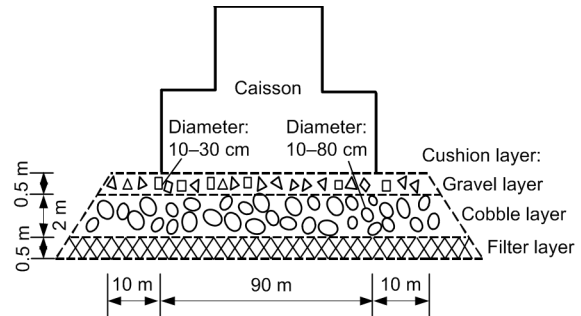


Fig. 1 Diagram of the gravel cushion used in the Rion-Antirion bridge

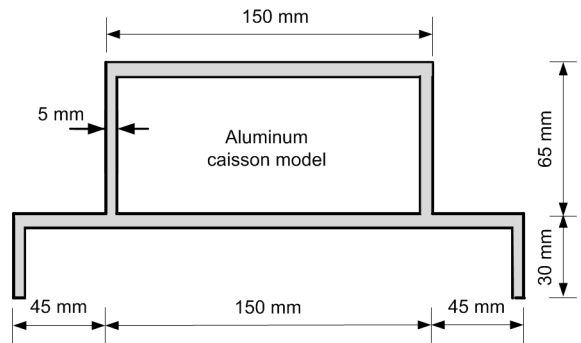


Fig. 2 Dimensions of the aluminum caisson model foundation

Table 1 Design of model scale

Model scale	Parameter	Value	
		Prototype	Model
Horizontal scale ($\lambda_L=1:375$)	Cushion layer	110.0	0.2933
	diameter (m)		
Vertical scale ($\lambda_H=1:300$)	Gravel layer	0.5	0.0017
	thickness (m)		
	Cobble layer	2.0	0.0067
	thickness (m)		
	Filter layer	0.5	0.0017
	thickness (m)		
Particle scale ($\lambda_d=1:145.5$)	Gravel	0.3	0.0021
	diameter (m)		
	Cobble	0.8	0.0055
	diameter (m)		



Fig. 3 Diagram of model foundation

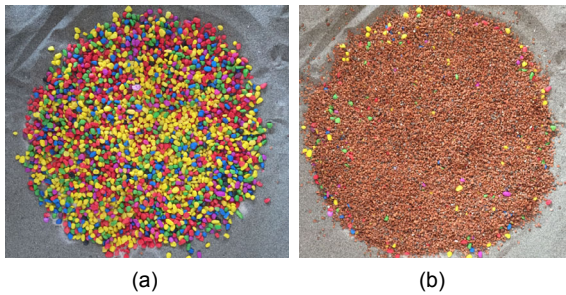


Fig. 4 Illustration of gravel cushion under the model foundation base
(a) Cobble layer; (b) Gravel layer

2.2 Laboratory tests set-up

A set-up for the horizontal vibration test is shown in Fig. 5. The test was conducted in a rectangular model container (1.5 m×1.0 m×1.0 m) with a rigid boundary wall made of glass. In order to minimize the reflection of the stress wave from the rigid boundary wall during the test, sponge was attached to the internal side of the model container. A steady-state sinusoidal force was generated by an electrodynamic exciter, and a force transducer was fixed between the exciter and caisson to record the excitation force during the test. The force transducer monitors whether the excitation force is consistent with the dynamic signal output from the computer. The dynamic response of the caisson foundation based on the cushion layer was measured using an acceleration sensor A1 connected to the top center of the caisson. The acceleration sensor A2 attached to the boundary was used to monitor the acceleration response of the model container. A data acquisition and analysis sys-

tem (DAS) consisting of a charge amplifier and a data acquisition analyzer (DAA) were used to monitor and record the time history of response of the caisson measured by the acceleration sensor. The dynamic displacement amplitude of the caisson could then be derived from the double integration of the acceleration recorded by the acceleration sensor.

The principal diagram of the harmonic vibration test is shown in Fig. 6. First, a harmonic sinusoidal vibration signal is output from the computer, and then that signal is transformed by the DAA and applied to the caisson foundation by the electrodynamic exciter. Finally, the acceleration sensor A1 automatically measures the dynamic response of the caisson and then feeds it back to the DAA and computer.

It is obvious that the dynamic load amplitude acting on the foundation is a very important factor for its response. Therefore, a static load-displacement test was carried out before the vibration test so as to make an appropriate selection of the dynamic force acting on the foundation. The multi-stage loading method was used in the static load test, and the test stopped when there was an obvious slippage between the foundation and the cushion layer.

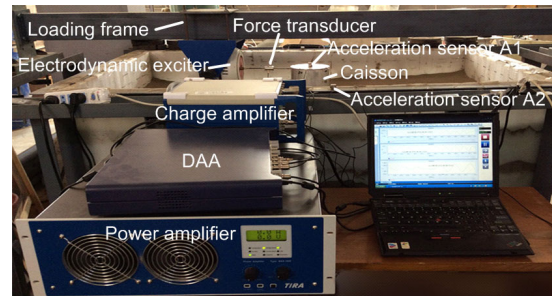
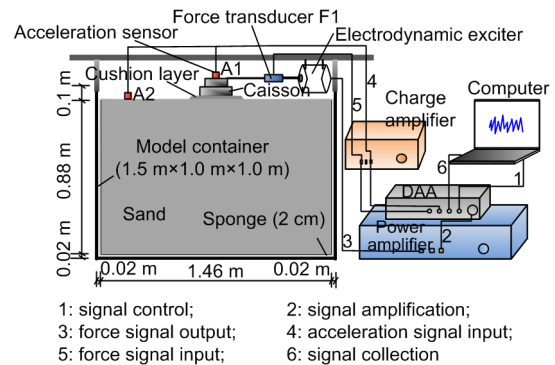


Fig. 5 Set-up for the horizontal vibration test



- 1: signal control;
- 2: signal amplification;
- 3: force signal output;
- 4: acceleration signal input;
- 5: force signal input;
- 6: signal collection

Fig. 6 Principal diagram of the harmonic vibration test

2.3 Test results and analysis

The static load-displacement curves of a caisson based on a gravel cushion and on a sand cushion are shown in Fig. 7. It is obvious that the horizontal displacement at the top of the caisson foundation increases as the load increases, and the displacement of the foundation suddenly increases when the load exceeds a certain value. That value, namely the horizontal ultimate bearing capacity (P_u), is mainly attributed to the frictional resistance between the foundation and the cushion layer. It can be found that the lateral bearing capacity of the caisson foundation based on the sand cushion is greater than that of the caisson foundation based on the gravel cushion. That is to say, a caisson based on a sand cushion is safer under static load than one based on a gravel cushion.

For the harmonic vibration test, the time history response of acceleration will continuously change with the increase of the load cycle as a larger dynamic load force is applied, and a suitable value should be selected. Here, the horizontal ultimate bearing capacity of the caisson is used as the reference. The sinusoidal lateral harmonic loads applied at the caisson top are 1, 2, 3, and 5 N which are about $0.05P_u$ – $0.23P_u$ of the caisson, where P_u is about 22 N.

Before the vibration test, the time histories of dynamic response recorded by the acceleration sensor and force transducer excitation by the environmental vibration are shown in Fig. 8. It can be seen that the effect of the environmental vibration is small, which implies that the current conditions are suitable for the vibration test. Equipment debugging was also carried out. Comparing the input excitation force signal from the computer and the output excitation force signal measured by the force transducer F1 at a frequency of 13 Hz, as shown in Fig. 9, it can be seen that the curve of input excitation force was coincided with that of the output excitation force, which shows the stability of the output signal.

A series of horizontal harmonic vibration tests were conducted on the caisson foundation based on the sand and gravel cushions. During the tests, the excitation force is gradually increased from $0.05P_u$ to $0.23P_u$. Since the resonant frequency of the caisson foundation cannot be known in advance, the frequency of the excitation force is increased from a low value until the peak of the response curve occurs.

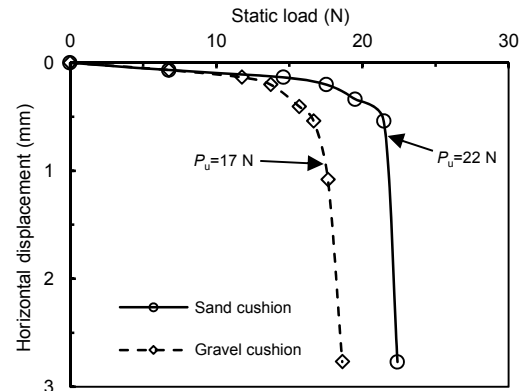


Fig. 7 Horizontal load-displacement curves of caisson foundation on different cushion types

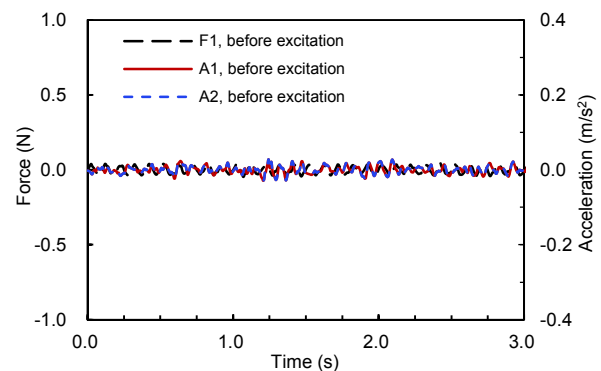


Fig. 8 Time histories of dynamic force and acceleration under environmental vibration

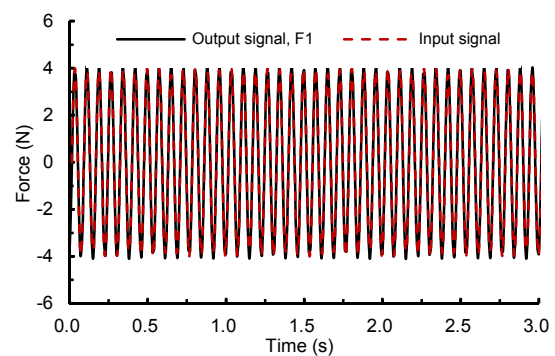


Fig. 9 Time histories of input signal and output signal

Typical time histories of the force and acceleration at the top of the caisson foundation based on the gravel cushion obtained from the force transducer and acceleration sensor are shown in Fig. 10. Here, the caisson was subjected to a sinusoidal harmonic excitation with frequency $f=37$ Hz, and the amplitude of excitation force output from the computer is 3 N. It can be seen that the input force signal is consistent

with the output force signal recorded by the force transducer, which shows the stability of the excitation load during the test. Compared with the value recorded by sensor A1, the acceleration value recorded by sensor A2 is very small, which indicates that the dynamic response of the caisson foundation induced by the environmental vibration and wave reflection is relatively small, and the response of caisson is less disturbed by the reflected waves. It can also be seen from Fig. 10 that the dynamic force and acceleration of the caisson undergo sinusoidal motion and that the acceleration lags behind the force due to the nonlinear damping effect of the soil. For the caisson based on the sand cushion and the gravel cushion under other loads and frequencies of excitation, the time history curves of the force and acceleration of the foundation are basically the same as those in Fig. 10, and thus are not listed here one by one.

The lateral dynamic responses of the top of the caisson under various harmonic excitation loads and different cushion types are measured by the model vibration test. The time history of dynamic displacement of the caisson is calculated by the double integration of acceleration, and the displacement amplitudes atop the foundation (u) at different excitation frequencies (f) are summarized, with the results shown in Figs. 11 and 12. The test results show that the resonant frequency of the foundation decreases as the magnitude of the excitation load increases both with the sand cushion and with the gravel cushion, indicating a nonlinear interaction due to the degradation of the stiffness of the soil and an increase of the damping effect. We can see that the rate of decrease of the resonance frequency of the caisson based on the gravel cushion is about twice that of the caisson based on the sand cushion, as shown in Table 2.

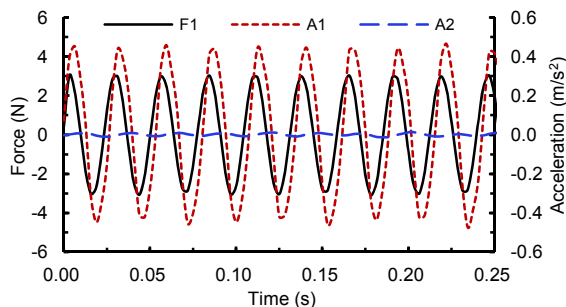


Fig. 10 Typical time histories of dynamic force and acceleration under lateral vibration

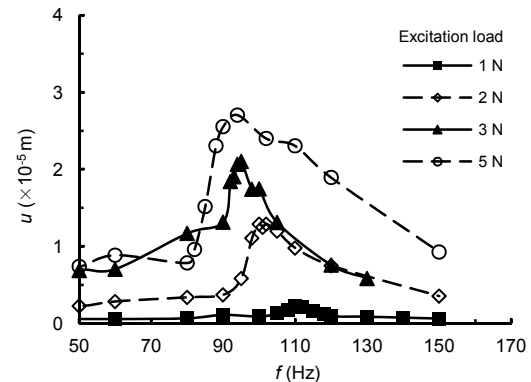


Fig. 11 Lateral dynamic response of caisson foundation on the sand cushion

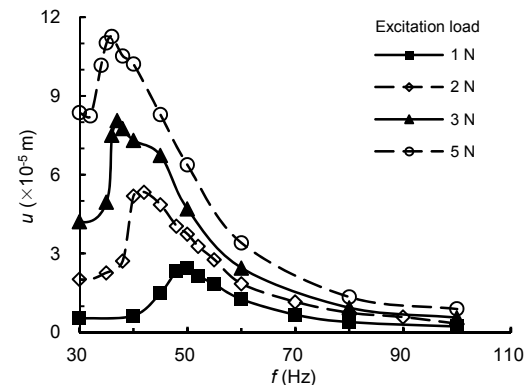


Fig. 12 Lateral dynamic response of caisson foundation on the gravel cushion

It is obvious that the displacement of the caisson increases significantly with the increase in the excitation load, and shows a typical nonlinear growth characteristic. The peak displacement amplitudes of caissons based on the gravel cushion and the sand cushion are also summarized in Table 2. The dynamic response of the caisson based on the gravel cushion is larger than that of the caisson based on the sand cushion. However, the rate of increase of the displacement amplitude of the caisson based on the sand cushion is similar to that of the caisson based on the gravel cushion. The foundation based on the gravel cushion is prone to a horizontal shear deformation under lateral or seismic loading, and the gravel cushion layer enters the plastic stage more quickly than the sand cushion layer when subjected to lateral vibration. This implies that the gravel cushion can dissipate the transmission of energy from the bottom part of the foundation, which in turn shows better vibration isolation performance than the sand cushion.

Table 2 Results of the model tests

Cushion	Load amplitude (N)	Resonant frequency (Hz)	Decrease rate in resonant frequency (%)	Peak displacement amplitude ($\times 10^{-5}$ m)	Increase rate in peak displacement amplitude (%)
Sand	1	110	–	0.6	–
	2	100	9.1	1.3	116.7
	3	95	13.6	2.2	266.7
	5	92	16.4	2.8	366.7
Gravel	1	50	–	2.4	–
	2	42	16.0	5.3	120.8
	3	37	26.0	8.1	237.5
	5	35	30.0	11.3	370.8

The gravel cushion layer can be equivalent to a plastic hinge to account for inelastic deformation and dissipation.

Considering that pure slip deformation between the foundation and the cushion layer is almost impossible, and the displacement amplitude of the foundation base is relatively small compared with that of the foundation top, it is assumed that the displacement generated by the horizontal excitation force at the top of the foundation is mainly attributable to the rotation angles of the foundation. Therefore, the vibration process can be considered as a rocking vibration of a rigid shallow foundation placed on the soil surface and, according to the theory of surface foundation vibration on an elastic half-space, the resonant frequency of the foundation is given by (Park et al., 2017)

$$f_r = \frac{1}{2\pi} \sqrt{\frac{K_{MM}}{I_0}} \sqrt{1 - 2D_s^2} = \frac{1}{2\pi} \sqrt{\frac{8Gr_0^3}{(1-\nu)I_0}} \sqrt{1 - 2D_s^2}, \quad (2)$$

where K_{MM} is the rocking stiffness of the surface foundation, I_0 is the mass moment of inertia of the caisson foundation, r_0 is the radius of the foundation base, and G , ν , and D_s are the shear modulus, Poisson's ratio, and damping ratio of the soil under the foundation, respectively.

According to the experimental results of the resonant frequency, summarized in Table 2, the equivalent shear modulus of the soil at the bottom of the foundation can be obtained by Eq. (2), as shown in Table 3. The results show that the equivalent shear modulus gradually decreases with the increase of the excitation force amplitude, which further proves that a nonlinear interaction occurs between the foundation and cushion layer during the vibration test. The

Table 3 Calculations of equivalent soil shear modulus

Cushion	Load amplitude (N)	Equivalent shear modulus (MPa)	Decrease rate in shear modulus (%)
Sand	1	1.63	–
	2	1.35	17.0
	3	1.22	24.7
	5	1.14	29.0
Gravel	1	0.34	–
	2	0.24	29.1
	3	0.19	44.7
	5	0.17	50.3

comparison shows that the equivalent shear modulus reduction rate of the gravel cushion is faster than that of the sand cushion.

3 Nonlinear lateral dynamic response analysis

3.1 Nonlinear analysis model

To demonstrate the lateral response of the caisson foundation under a harmonic excitation force, the dynamic equilibrium equation of the caisson based on the Winkler model can be expressed as (Gerolymos and Gazetas, 2006)

$$\mathbf{K} \begin{Bmatrix} u_b \\ \theta \end{Bmatrix} = (-\omega^2 \mathbf{M}_b + \mathbf{K}_b) \begin{Bmatrix} u_b \\ \theta \end{Bmatrix} = \mathbf{P}_b, \quad (3)$$

where \mathbf{K} is the dynamic impedance matrix of the foundation, \mathbf{P}_b is the load vector, \mathbf{M}_b is the mass matrix of the foundation, \mathbf{K}_b is the complex stiffness of the foundation, ω is the circular frequency, and u_b and θ are the horizontal displacement and the rotation angle of the base center of the foundation, respectively.

$$\mathbf{P}_b = \left\{ \begin{array}{c} Q_0 \\ DQ_0 + M_0 \end{array} \right\}, \quad (4)$$

$$\mathbf{M}_b = \begin{bmatrix} m & D_1 m \\ D_1 m & J + D_1^2 m \end{bmatrix}, \quad (5)$$

$$\mathbf{K} = \begin{bmatrix} K_{HH} + i\omega C_{HH} & K_{HM} + i\omega C_{HM} \\ K_{MH} + i\omega C_{MH} & K_{MM} + i\omega C_{MM} \end{bmatrix}, \quad (6)$$

$$\mathbf{K}_b = \begin{bmatrix} \bar{K}_{HH} & \bar{K}_{HM} \\ \bar{K}_{MH} & \bar{K}_{MM} \end{bmatrix}, \quad (7)$$

where Q_0 and M_0 are the harmonic lateral vibration load and the moment acting on the top of the foundation, respectively. D is the height of the foundation, and D_1 is the distance between the center of gravity and the base surface of the caisson. m and J are the mass and mass moment of inertia of the caisson. K_{HH} , K_{HM} , K_{MH} , and K_{MM} are the horizontal stiffness, horizontal-rocking stiffness, rocking-horizontal stiffness, and rocking stiffness of the foundation, respectively. C_{HH} , C_{HM} , C_{MH} , and C_{MM} are the horizontal damping, horizontal-rocking damping, rocking-horizontal damping, and rocking damping of the foundation, respectively. Based on the surface foundation theory, \bar{K}_{HH} , \bar{K}_{HM} , \bar{K}_{MH} , and \bar{K}_{MM} are given as (Gazetas, 1991; Zhong and Huang, 2013):

$$\bar{K}_{HH} = \xi \frac{8Gr_0^2}{2-\nu} + i\omega \frac{16Gr_0^2}{5V_s}, \quad (8)$$

$$\bar{K}_{MM} = \eta \frac{8Gr_0^3}{3(1-\nu)} + i\omega \frac{4Gr_0^4}{5(1-\nu)V_s}, \quad (9)$$

$$\bar{K}_{HM} = \bar{K}_{MH} = 0, \quad (10)$$

$$\eta = 1 - 0.3 \frac{\omega r_0}{V_s}, \quad (11)$$

where ξ and η are the horizontal dynamic coefficient and the rocking dynamic coefficient, respectively. For the surface foundation, ξ is equal to 1 (Gazetas and Tassoulas, 1987). V_s is the shear wave velocity of the soil.

Since the soil nonlinearity lasted for the whole process of vibration test, the elastic model proposed by Gerolymos and Gazetas (2006) is not suitable for the test analysis. Here, the Hardin-Drnevich model (Hardin and Drnevich, 1972) was employed to rep-

resent the nonlinear soil reactions within the frame of the Winkler model mentioned above (Gerolymos and Gazetas, 2006).

$$\frac{G}{G_0} = \frac{1}{1 + \gamma/\gamma_r}, \quad (12)$$

$$D_s = D_{smax} (1 - G/G_0), \quad (13)$$

$$\gamma_r = \tau_f / G_0, \quad (14)$$

where G_0 is the initial shear modulus of soil, which is mainly related to the mean effective stress σ_m and void ratio e of soil (Yang and Gu, 2013). γ is the shear strain of soil, γ_r is the reference shear strain, D_{smax} is the maximum value of the damping ratio, and τ_f is the shear stress at failure.

In order to obtain the dynamic response of the foundation, the most important thing is to determine G_0 . According to the previous assumption that the displacement is mainly caused by the rotation angle, the equivalent shear strain of soil at the foundation base can be calculated according to that displacement (Kagawa and Kraft, 1980). Then, the equivalent G_0 can be obtained from Eq. (12), as shown in Fig. 13. The equivalent G_0 of the sand cushion and the gravel cushion are 1.9 MPa and 0.55 MPa, respectively. Finally, considering the change rule of the dynamic shear modulus and damping ratio with the soil strain, the nonlinear dynamic response of the caisson foundation can be obtained by an iterative method, as follows:

Step 1: Assume the initial displacement of the foundation is zero. The initial shear modulus G_0 and D_{smax} are determined by the laboratory test or the empirical method (Hardin and Drnevich, 1972).

Step 2: According to the excitation force acting on the foundation, calculate the current average shear strain of soil γ^i , which can be determined by the displacement of the foundation u_b^i and θ^i (Kagawa and Kraft, 1980). Then, the shear modulus G^i and damping ratio D_s^i can be obtained by Eqs. (12) and (13).

Step 3: The complex stiffness of the foundation \mathbf{K}_b^i is modified by the current shear modulus G^i and damping ratio D_s^i .

Step 4: According to the updated value of \mathbf{K}_b^i , the average shear strain γ^{i+1} , the shear modulus G^{i+1} , and the damping ratio D_s^{i+1} can be obtained. This

process is repeated until the required convergence criteria for the solution are met.

Fig. 14 is a flow chart illustrating the analysis process of the nonlinear dynamic Winkler model proposed above to analyze the dynamic response of a laterally loaded caisson foundation.

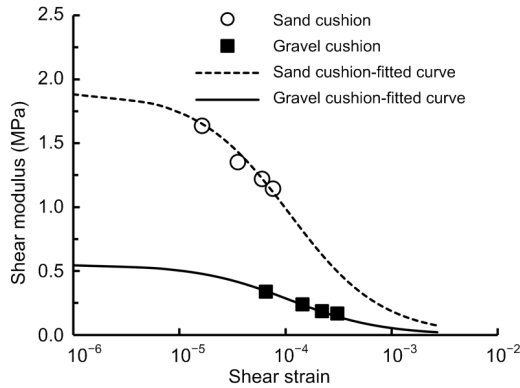


Fig. 13 Shear modulus-strain relationships of the sand cushion and the gravel cushion

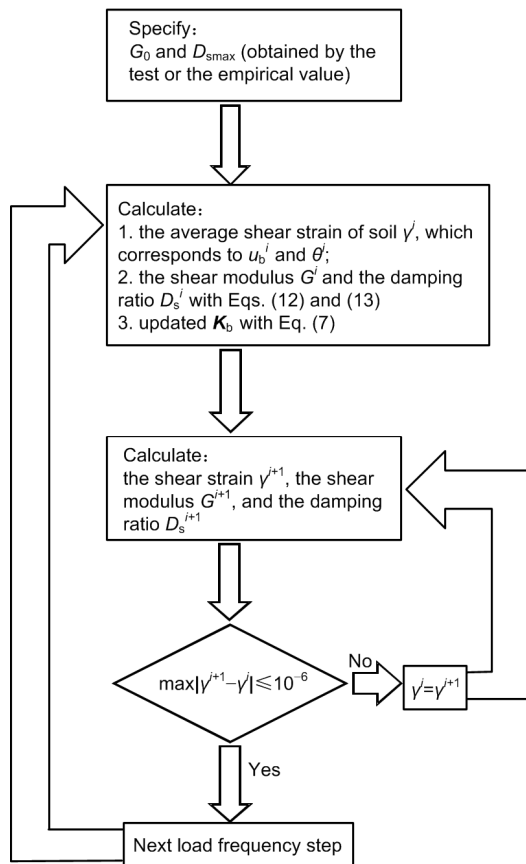


Fig. 14 Flow chart for the nonlinear analysis

3.2 Comparison against the test results

Compared with the experimental results, the lateral dynamic displacement responses of caissons based on sand and gravel cushions and considering soil nonlinearity as a function of the frequency f , are shown in Figs. 15 and 16, respectively. The horizontal displacement of the foundation based on the cushion layer has a deviation between the experimental results and the predicted response, especially under a relatively large load. The maximum deviations of horizontal displacement of the sand cushion and of the gravel cushion are near the resonant frequency. Two factors may contribute to these deviations:

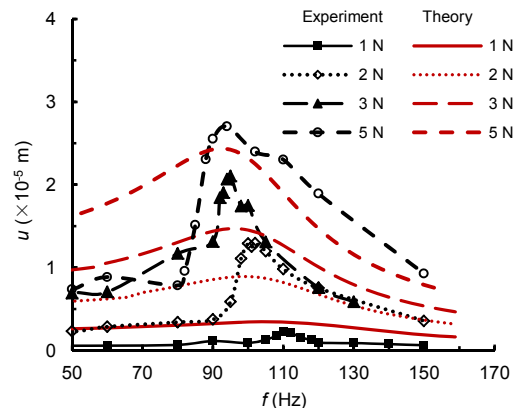


Fig. 15 Comparison of the lateral dynamic response of caisson foundation on the sand cushion

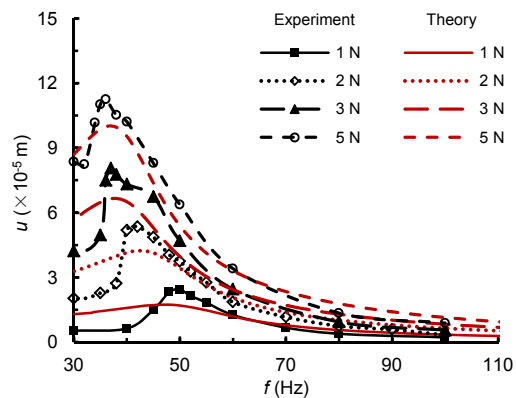


Fig. 16 Comparison of the lateral dynamic response of caisson foundation on the gravel cushion

1. There is no specific guideline available to determine the shear modulus of the soil under the foundation. The equivalent shear modulus of the cushion layer was used in this analysis and it may cause a difference in displacement amplitude compared with the real model. However, the displacement

amplitude in the high-frequency range has a reasonable match with the experimental results. Thus, the mass of the foundation may play a controlling role in the high-frequency range.

2. The dynamic response of the foundation is closely related to the nonlinear characteristics of the interface between the foundation base and cushion layer, especially for a relatively large load acting on the foundation (Mortara et al., 2002). However, only the soil nonlinearity under the foundation base is considered in this study, and the changes in the dynamic characteristics of the foundation caused by the changes of the characteristics of that interface have not been taken into account. The nonlinearity of the interface increases with the increase of the excitation force, which will affect the dynamic response of the foundation.

To further investigate their rocking characteristics, the rocking displacement responses of the foundations are also calculated by the proposed method, with the results shown in Figs. 17 and 18. It can be seen that the shapes of the rocking displacement response have similar trends to those of the horizontal displacement. It can be also found that the horizontal displacement amplitudes of the foundation at different excitation forces are small compared to the rotation angles. The displacement at the top of the caisson foundation is mainly caused by the rotation (the height of the caisson is equal to 95 mm), which is consistent with the assumption mentioned above.

Figs. 19 and 20 show the dynamic impedance of the foundation based on the sand cushion under different excitation forces. It can be observed that the effect of the excitation force reduces the horizontal impedance and the rocking impedance. However, the decrease in dynamic horizontal and rocking stiffness is less at the high-frequency range, where it can be negligible, and the reduction in horizontal damping and rocking damping is clear for different frequencies of excitation force. Furthermore, similar trends can also be seen in Figs. 21 and 22 for the horizontal impedance and rocking impedance of the caisson foundation based on the gravel cushion.

In general, the predicted dynamic response of a foundation based on a cushion layer has a reasonable match with the experimental results despite the simplicity of the proposed model. However, it should be pointed out that the thickness of the cushion layer and

the overburden pressure acting on the foundation base also have impacts on the dynamic characteristics of the foundation (Zhao et al., 2016; Chen et al., 2018). The selection of the soil parameters here is oriented toward qualitative analysis. Dynamic triaxial tests or resonant column tests are needed to determine the shear modulus before engineering applications, and the effective depth of soil should be further studied. In addition, the dynamic response of the foundation based on the cushion layer shows a nonlinear growth trend, especially when the excitation force is large. Therefore, the dynamic characteristics of a foundation influenced by interaction at the interface must also be further investigated.

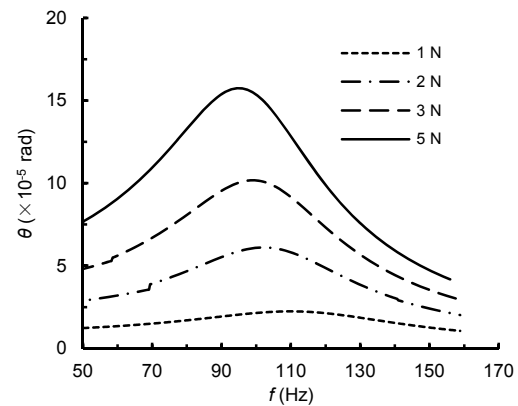


Fig. 17 Rotation angles of caisson foundation on the sand cushion

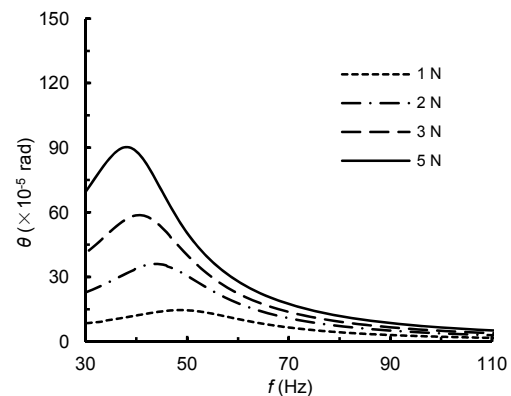


Fig. 18 Rotation angles of caisson foundation on the gravel cushion

4 Discussion

The relationship between the model and prototype foundation is also a common concern. As

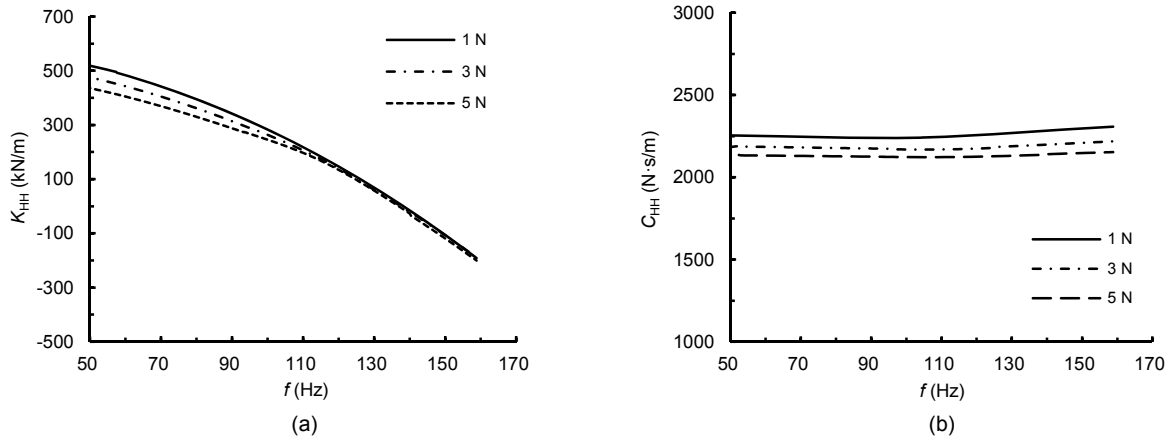


Fig. 19 Horizontal impedance of caisson foundation on the sand cushion
 (a) Horizontal stiffness; (b) Horizontal damping

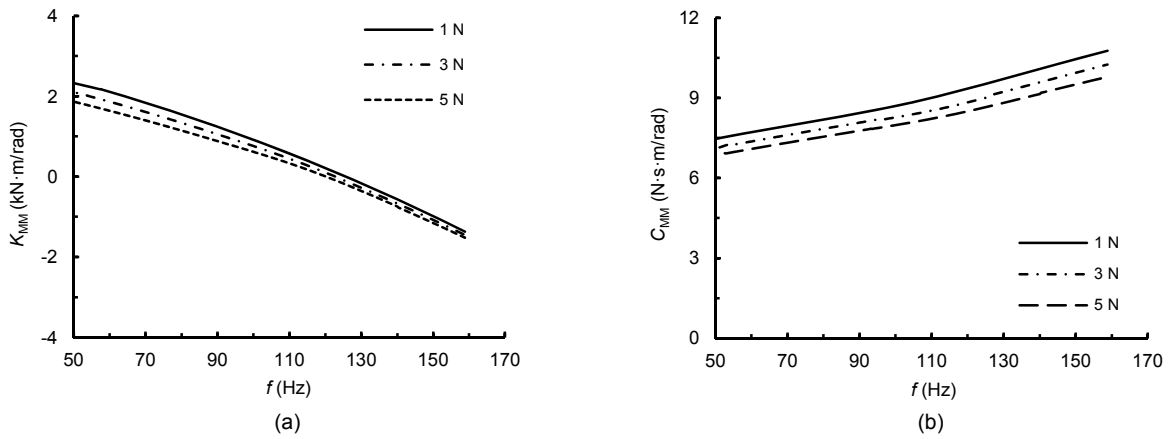


Fig. 20 Rocking impedance of caisson foundation on the sand cushion
 (a) Rocking stiffness; (b) Rocking damping

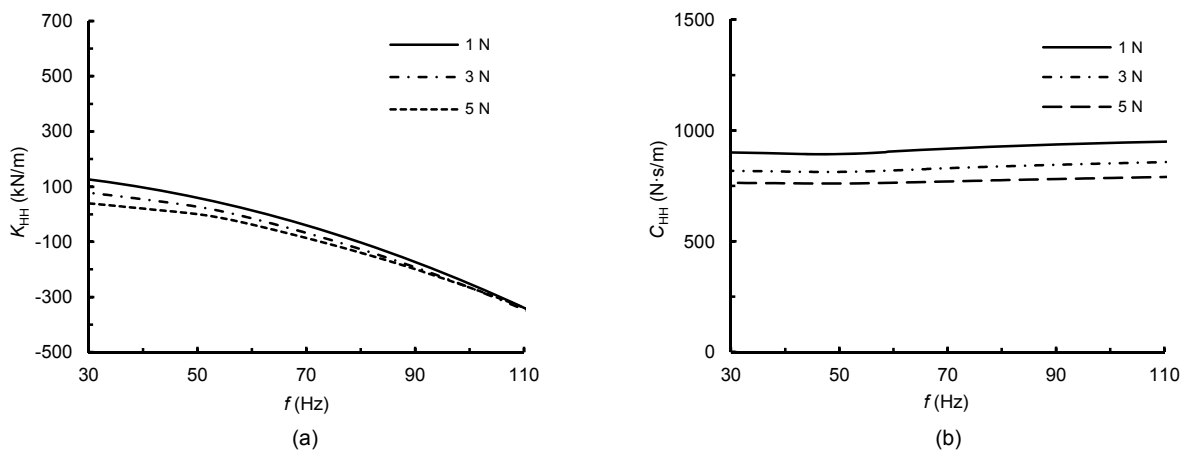


Fig. 21 Horizontal impedance of caisson foundation on the gravel cushion
 (a) Horizontal stiffness; (b) Horizontal damping

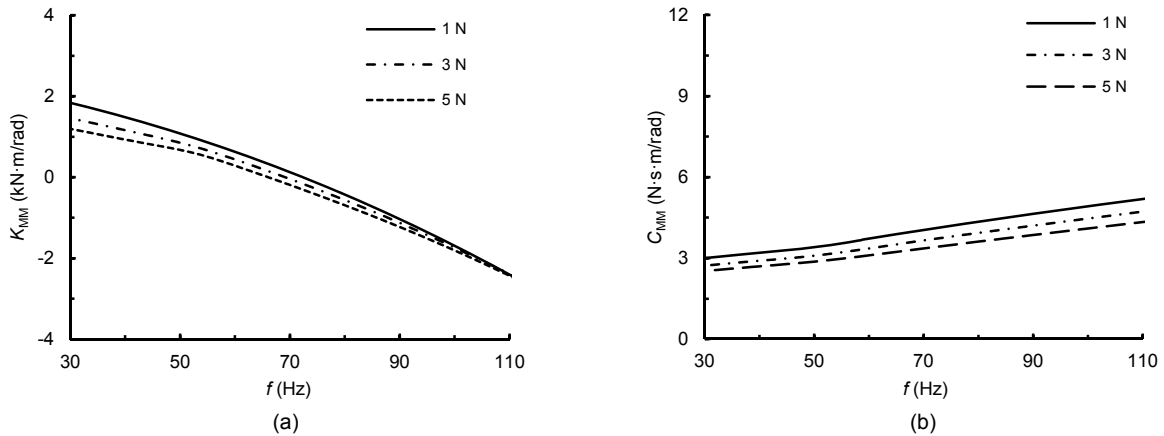


Fig. 22 Rocking impedance of caisson foundation on the gravel cushion
(a) Rocking stiffness; (b) Rocking damping

mentioned above, λ_N and λ_p are equal to 375 and 1.0, respectively. λ_e is equal to $\lambda_N[(V_s)_m/(V_s)_p]^2$, namely $\lambda_N[(G_0)_m/(G_0)_p]$, where $(G_0)_m$ and $(G_0)_p$ are the shear moduli of soil in the model and the prototype, respectively. $(G_0)_m$ used in the model test is shown in Fig. 13. Empirically, we can assume that $(G_0)_m/(G_0)_p$ approximately equals 1/375, namely $\lambda_e=1.0$. Then, in the case of this small-scale model, all the other scaling factors can be determined by the scaling factors for length λ_N , density λ_p , and strain λ_e (Iai et al., 2005; Park and Kim, 2013). The scaling factors for 1g model tests are reproduced in Table 4.

Table 4 Scaling factors for 1g model test (Iai et al., 2005)

Item	Scaling factor for 1g model test	Scaling factor in this study ($\lambda_p=1, \lambda_e=1$)
Length	λ_N	λ_N
Density	λ_p	1
Strain	λ_e	1
Stiffness	$\lambda_N \cdot \lambda_p / \lambda_e$	λ_N
Time	$(\lambda_N \cdot \lambda_e)^{0.5}$	$\lambda_N^{0.5}$
Frequency	$(\lambda_N \cdot \lambda_e)^{-0.5}$	$\lambda_N^{-0.5}$

According to the scaling factors listed in Table 4, the resonant frequency of the $1/\lambda_N$ model is $\lambda_N^{0.5}$ times the resonant frequency of the prototype, and it is consistent with the results of Eq. (2) if scaling factors for G (λ_N) and I_0 (λ_N^4) are substituted. Then, the resonant frequency of the prototype foundation can be calculated by the scaling factors, as shown in Table 5. It should be noted that the selection of the shear

modulus of soil here is oriented toward qualitative analysis. The shear modulus of soil is very important for the dynamic response in theoretical analysis and engineering practice. Therefore, in-situ test, dynamic triaxial test, or resonant column test should be conducted to determine the soil parameters before engineering application.

Table 5 Resonant frequencies of the model and the prototype foundation

Cushion	Load amplitude (N)	Resonant frequency of model (Hz)	Resonant frequency of prototype (Hz)
Sand	1	110	5.68
	2	100	5.16
	3	95	4.91
	5	92	4.75
Gravel	1	50	2.58
	2	42	2.17
	3	37	1.91
	5	35	1.81

5 Conclusions

A comprehensive study, involving both dynamic laboratory tests and theoretical analysis, to investigate the nonlinear dynamic characteristics of a laterally loaded caisson foundation based on a cushion layer is presented. Two series of tests under various excitation forces are conducted to study the effect of the cushion type on the nonlinear dynamic response of the foundation, and the dynamic behavior of the prototype

foundation is discussed using the results from a small-scale model in 1g model test. The following conclusions can be drawn:

1. During the static loading test, the displacement of the foundation based on the sand cushion or gravel cushion increases along an ideal elastic-plastic curve with the increase of load. The displacement of the foundation suddenly increases when the load exceeds the ultimate bearing capacity, and the ultimate bearing capacity of the foundation based on the sand cushion is larger than that of the foundation based on the gravel cushion.

2. Due to the soil nonlinearity, the time history response of acceleration lags behind the time history of the excitation force, and the displacement of the foundation shows a nonlinear growth trend with the increase of the excitation force, while the resonant frequency gradually decreases.

3. The dynamic response of the caisson based on the gravel cushion is significantly larger than that of the caisson based on the sand cushion, and the rate of decrease of resonant frequency of a foundation based on the gravel cushion is faster than that of foundation based on the sand cushion under the same conditions. The gravel cushion shows better vibration isolation performance than the sand cushion as the gravel cushion can more effectively dissipate the energy from the bottom part of the foundation.

4. The simplified analysis method can effectively simulate the dynamic response of the caisson foundation based on the cushion layer. Considering the complexity and diversity of the soil, more research is needed, and further optimization is also needed to consider the effect of the interface characteristics on the dynamic response.

5. According to the scaling factors for 1g model tests, the relationships between the model and the prototype foundation are closely related to the shear modulus of soil. Therefore, in-situ test, dynamic triaxial test, or resonant column test should be conducted to obtain the soil parameters before engineering application.

Contributors

Mao-song HUANG designed the research. Wen-bo TU processed the corresponding data and wrote the first draft of the manuscript. Xiao-qiang GU helped to organize the manuscript. Wen-bo TU revised and edited the final version.

Conflict of interest

Wen-bo TU, Mao-song HUANG, and Xiao-qiang GU declare that they have no conflict of interest.

References

- Chen YW, Huang MS, Lou CY, 2018. Model tests and analyses of caisson foundation based on gravel cushion under cyclic lateral loads. *Chinese Journal of Geotechnical Engineering*, 40(9):1619-1626 (in Chinese).
<https://doi.org/10.11779/CJGE201809007>
- Combault J, 2011. The Rion-Antirion bridge—when a dream becomes reality. *Frontiers of Architecture and Civil Engineering in China*, 5(4):415-426.
<https://doi.org/10.1007/s11709-011-0130-x>
- Combault J, Morand P, Pecker A, 2000. Structural response of the Rion-Antirion bridge. Proceedings of the 12th World Conference on Earthquake Engineering, p.1609.
- Dong XW, Zhou SZ, 2004. Design and construction of Rion-Antirion bridge in Greece. *World Bridges*, (4):1-4 (in Chinese).
<https://doi.org/10.3969/j.issn.1671-7767.2004.04.001>
- Dou GR, 2001. Similarity theory of total sediment transport modeling for estuarine and coastal regions. *Hydro-Science and Engineering*, 1(1):1-12 (in Chinese).
<https://doi.org/10.3969/j.issn.1009-640X.2001.01.001>
- Gazetas G, 1991. Formulas and charts for impedances of surface and embedded foundations. *Journal of Geotechnical Engineering*, 117(9):1363-1381.
[https://doi.org/10.1061/\(asce\)0733-9410\(1991\)117:9\(1363\)](https://doi.org/10.1061/(asce)0733-9410(1991)117:9(1363))
- Gazetas G, Tassoulas JL, 1987. Horizontal stiffness of arbitrarily shaped embedded foundations. *Journal of Geotechnical Engineering*, 113(5):440-457.
[https://doi.org/10.1061/\(asce\)0733-9410\(1987\)113:5\(440\)](https://doi.org/10.1061/(asce)0733-9410(1987)113:5(440))
- Gerolymos N, Gazetas G, 2006. Winkler model for lateral response of rigid caisson foundations in linear soil. *Soil Dynamics and Earthquake Engineering*, 26(5):347-361.
<https://doi.org/10.1016/j.soildyn.2005.12.003>
- Ghalesari AT, Rasouli H, 2014. Effect of gravel layer on the behavior of piled raft foundations. Proceedings of Geo-Shanghai 2014, p.373-382.
<https://doi.org/10.1061/9780784413425.038>
- Gu XQ, Yang J, Huang MS, et al., 2015. Bender element tests in dry and saturated sand: signal interpretation and result comparison. *Soils and Foundations*, 55(5):951-962.
<https://doi.org/10.1016/j.sandf.2015.09.002>
- Hall L, Bodare A, 2000. Analyses of the cross-hole method for determining shear wave velocities and damping ratios. *Soil Dynamics and Earthquake Engineering*, 20(1-4): 167-175.
[https://doi.org/10.1016/S0267-7261\(00\)00048-8](https://doi.org/10.1016/S0267-7261(00)00048-8)
- Han XL, Li YK, Ji J, et al., 2016. Numerical simulation on the seismic absorption effect of the cushion in rigid-pile composite foundation. *Earthquake Engineering and Engineering Vibration*, 15(2):369-378.
<https://doi.org/10.1007/s11803-016-0329-x>

- Hardin BO, Drnevich VP, 1972. Shear modulus and damping in soils: design equations and curves. *Journal of the Soil Mechanics and Foundations Division*, 98(7):667-692.
- Iai S, Sugano T, 1999. Soil-structure interaction studies through shaking table tests. Proceedings of the 2nd International Conference on Earthquake Geotechnical Engineering, p.927-940.
- Iai S, Tobita T, Nakahara T, 2005. Generalised scaling relations for dynamic centrifuge tests. *Géotechnique*, 55(5):355-362.
https://doi.org/10.1680/geot.2005.55.5.355
- Infanti S, Papanikolas P, Benzoni G, et al., 2004. Rion-Antirion bridge: design and full-scale testing of the seismic protection devices. Proceedings of the 13th World Conference on Earthquake Engineering, p.2174-2189.
- Kagawa T, Kraft LM, 1980. Lateral load-deflection relationships of piles subjected to dynamic loadings. *Soils and Foundations*, 20(4):19-36.
https://doi.org/10.3208/sandf1972.20.4_19
- Li L, 1989. Seismic Isolation and Absorption Technology. Seismological Press, Beijing, China (in Chinese).
- Liang FY, Chen LZ, Shi XG, 2003. Numerical analysis of composite piled raft with cushion subjected to vertical load. *Computers and Geotechnics*, 30(6):443-453.
https://doi.org/10.1016/S0266-352X(03)00057-0
- Liu FC, Wu MT, Chen JL, et al., 2017. Experimental study on influence of geo-cell reinforcement on dynamic properties of rubber-sand mixture. *Chinese Journal of Geotechnical Engineering*, 39(9):1616-1625 (in Chinese).
https://doi.org/10.11779/CJGE201709009
- Mortara G, Boulon M, Ghionna VN, 2002. A 2-D constitutive model for cyclic interface behaviour. *International Journal for Numerical and Analytical Methods in Geomechanics*, 26(11):1071-1096.
https://doi.org/10.1002/nag.236
- Park HJ, Kim DS, 2013. Centrifuge modelling for evaluation of seismic behaviour of stone masonry structure. *Soil Dynamics and Earthquake Engineering*, 53:187-195.
https://doi.org/10.1016/j.soildyn.2013.06.010
- Park HJ, Ha JG, Kwon SY, et al., 2017. Investigation of the dynamic behaviour of a storage tank with different foundation types focusing on the soil-foundation-structure interactions using centrifuge model tests. *Earthquake Engineering & Structural Dynamics*, 46(14):2301-2316.
https://doi.org/10.1002/eqe.2905
- Pecker A, 2004. Design and construction of the Rion Antirion bridge. Proceedings of Geo-Trans 2004, p.216-240.
https://doi.org/10.1061/40744(154)7
- Pecker A, Teyssandier JP, 1998. Seismic design for the foundations of the Rion Antirion bridge. *Proceedings of the Institution of Civil Engineers-Geotechnical Engineering*, 131(1):4-11.
https://doi.org/10.1680/igeng.1998.30001
- Qian JZ, 2004. Rion-Antirion bridge crossing the gulf of Corinth in Greece. *Technology of Highway and Transport*, (1):102-105 (in Chinese).
https://doi.org/10.3969/j.issn.1009-6477.2004.01.028
- Shang SP, Zhou ZJ, Liu K, et al., 2009. The research on the steel-asphalt isolation lay. *Journal of Railway Science and Engineering*, 6(3):13-16 (in Chinese).
https://doi.org/10.3969/j.issn.1672-7029.2009.03.003
- Wang C, Yu X, Liang FY, 2017. Erosion mechanism of local scour around cushioned caisson on reinforced ground. *Marine Georesources & Geotechnology*, 35(7):1028-1036.
https://doi.org/10.1080/1064119X.2016.1278567
- Yang J, Gu XQ, 2013. Shear stiffness of granular material at small strains: does it depend on grain size? *Géotechnique*, 63(2):165-179.
https://doi.org/10.1680/geot.11.P.083
- Zhao X, Zhang Q, Zhang Q, et al., 2016. Numerical study on seismic isolation effect of gravel cushion. Proceedings of the 7th International Conference on Discrete Element Methods, p.1055-1063.
- Zhong R, Huang MS, 2013. Winkler model for dynamic response of composite caisson-piles foundations: lateral response. *Soil Dynamics and Earthquake Engineering*, 55:182-194.
https://doi.org/10.1016/j.soildyn.2013.09.017
- Zhu JM, Zhang RX, Mu BG, et al., 2014. Application of gravel cushion in super-large laying-down foundations. *Highway*, 59(3):84-87 (in Chinese).

中文概要

题目: 不同垫层型式沉箱基础的水平振动特性研究

目的: 沉箱底部垫层型式对基础的水平振动特性有重要影响。本文旨在探讨不同垫层型式(砂垫层或碎石垫层)对沉箱基础水平动力响应的影响规律,并提出简化的沉箱垫层基础水平动力的非线性分析计算方法。

创新点: 1. 针对不同垫层下的沉箱基础开展室内水平稳态振动模型的试验研究; 2. 建立沉箱垫层基础的非线性分析计算模型; 3. 建立沉箱垫层基础模型的动力特性与原型沉箱垫层基础动力特性之间的关系。

方法: 1. 通过室内水平稳态振动模型试验研究, 得出不同垫层型式对沉箱基础动力特性的影响规律(图11和12); 2. 通过理论推导, 构建激振力大小与基础振动位移幅值及共振频率之间的关系, 并建立相应分析模型(公式(3)和(12)); 3. 通过相似理论, 分析模型基础与原型基础之间的动力特性关系(表5)。

结 论: 1. 静荷载作用下, 基础水平荷载-位移曲线近似于刚塑性发展过程, 且基础置于砂垫层时的极限荷载比置于碎石垫层的更大; 2. 沉箱置于砂垫层或碎石垫层上时, 随着激振力幅值的增大, 由于土体非线性特性的产生, 基础振动响应幅值明显增大, 且基础的共振频率呈衰减趋势; 3. 相对于砂

垫层, 碎石垫层在动力荷载作用下更易产生塑性变形, 从而消耗并阻隔部分能量的传递, 进而表现出比砂垫层更好的隔震效应。

关键词: 非线性动力响应; 沉箱基础; 稳态激振试验; 碎石垫层; 砂垫层